

Design PID Controllers Using Generalized Laguerre Functions

Vilem KARSKY¹, Martin TUMA²

¹ Dept. of Control and Instrumentation, Brno University of Technology, Technicka 12, 612 00 Brno, Czech Republic

² Central European Institute of Technology, Brno University of Technology, Technicka 12, 616 00 Brno, Czech Republic

karsky@vutbr.cz, martin.tuma@ceitec.vutbr.cz

Submitted December 22, 2021 / Accepted May 23, 2022 / Online first August 3, 2022

Abstract. *This paper deals with a method of designing PID controllers. Generalized Laguerre functions were used for this task. Generalized Laguerre functions generate an orthogonal base in the time domain and the operator domain. This property of generalized Laguerre functions is beneficially used for the design of the PID controller. Parameters for generalized Laguerre function PID controllers are computed from the Laguerre series of the open loop and the Laguerre series of the ideal open loop. To satisfy this goal, the plant transfer function, the controller transfer function, and the ideal open loop transfer function are transformed into a generalized Laguerre functions base. Three examples are shown to present this method.*

Keywords

PID controller, PI controller, PD controller, fractional order systems, generalized Laguerre functions, orthogonal functions

1. Introduction

Great development of modern approaches in control theory such as adaptive or robust control has been made recently. A summary and current developments can be found in a recently published summary article [1]. Despite these great advances in modern control theory the traditional approach to control using proportional-integral-derivative (PID) controllers still has its place in theoretical and practical applications. PID controllers are widely used in industrial applications. This is mainly due to the simple control structure while using PID controller and clear physical meaning of its parameters. Due to the long history of their application in the industry, their users have much experience in tuning up their parameters. A comprehensive discussion of PID controllers can be found, for example, in the book [2]. Due to the properties of PID controllers, their research is still a actual topic and many new publications can be found in the control theory literature, e.g. [3–6].

The history of using the Laguerre orthonormal functions in system modeling and identification since their introduction in [7] and [8] is rather long, with many papers documenting the differing theoretical approaches.

Simple Laguerre functions (SLFs) have some properties which could be beneficial in control applications. These SLFs have found application mainly in the system modeling and the system identification, as can be seen for example in [9–13]. However, they could also be used for the PID controllers design, as shown in [14], [15]; this usage of SLFs is not that common. Generalized Laguerre functions (GLFs) [16–18] generalize SLFs and offer one extra free parameter that could be used to obtain better results.

The application of GLFs with generalization parameter α instead of SLFs in system control theory is quite a new topic. The applications of GLFs can be found in the field of theoretical mathematics, see [19], [20], but these functions definitely deserve more attention in the control theory field. The identification method based on GLFs was introduced in [21]. This method was further compared with least squares based identification with state variable filters (LSSVF) in [22]. The advantage of the optimal choice of the free parameters in GLFs and its influence on the quality of identification was presented. Another example of the generalization of the SLFs method is the application of GLFs to the dead time estimation problem in [23]. This approach is an extension of SLFs based dead time estimation, which can be found in [24]. It was shown that thanks to the optimal choice of free parameters, it is possible to use a smaller number of members of the Laguerre approximation series for dead times. There is still much space for improvement of SLFs based algorithms in control theory with GLFs based approach.

This paper deals with employing GLFs to design PID controllers. This method utilizes the GLFs property to generate the orthogonal base. The open loop transfer function is transformed into the GLFs base and the first three coefficients of the spectrum are compared with the first three coefficients of the spectrum of the ideal open loop transfer function transformed into the GLFs base. This method can be also used

for fractional-order systems. In Sec. 2 the terminology for later parts of the paper is established. Definition of GLFs and their properties are introduced. A method how to use GLFs to design PID controllers is described in Sec. 3. Three examples to evaluate the method proposed in section are presented in Sec. 4. The results are compared with the method based on SLFs and with MATLAB pidtune method. Sec. 5 concludes this paper.

2. Basic Terms

This section outlines some basic terms which will be used later in this paper.

2.1 Generalized Laguerre Functions

GLFs are based on generalized Laguerre polynomials. Generalized Laguerre polynomials are defined according to [16–18, 25–27] as

$$L_n^\alpha(x) = \frac{e^x x^{-\alpha}}{n!} \frac{d^n}{dx^n} (x^{n+\alpha} e^{-x}). \quad (1)$$

They generate an orthogonal base in the time domain and also in the operator domain. They satisfy the equation

$$\int_0^\infty \frac{2\lambda m!}{\Gamma(m+\alpha+1)} (2\lambda t)^\alpha e^{-(2\lambda t)} L_n^\alpha(2\lambda t) L_m^\alpha(2\lambda t) dt = \delta_{mn} \quad (2)$$

where δ_{mn} is the Kronecker delta defined by

$$\delta_{mn} = \begin{cases} 0 & \text{if } m \neq n, \\ 1 & \text{if } m = n, \end{cases} \quad (3)$$

and $\Gamma(z)$ is Gamma function defined according to [28] by

$$\Gamma(z) = \int_0^\infty t^{z-1} e^{-t} dt. \quad (4)$$

GLFs could be extracted from (2) as

$$l_n^\alpha(2\lambda t) = \sqrt{\frac{2\lambda m!}{\Gamma(m+\alpha+1)}} (2\lambda t)^{\frac{\alpha}{2}} e^{-(\lambda t)} L_n^\alpha(2\lambda t). \quad (5)$$

For GLFs applies that

$$\langle l_n^\alpha(2\lambda t), l_m^\alpha(2\lambda t) \rangle = \delta_{mn} \quad (6)$$

where $\langle f, g \rangle$ means the scalar product of functions f and g .

For $\alpha = 0$, GLFs become SLFs. These GLFs generate an orthogonal base both in the time domain and the operator domain the same way as generalized Laguerre polynomials. Therefore any function $f(t) \in L_2$ could be represented as

$$f(t) = \sum_{n=0}^\infty c_n l_n^\alpha(2\lambda t) \quad (7)$$

and also

$$\mathcal{L}\{f(t)\} = \sum_{n=0}^\infty c_n \mathcal{L}\{l_n^\alpha(2\lambda t)\} \quad (8)$$

where $\mathcal{L}\{f(t)\}$ means Laplace transform of function $f(t)$.

Spectrum coefficients in (7) and (8) could be computed as

$$c_n = \langle f(t), l_n^\alpha(2\lambda t) \rangle = \langle \mathcal{L}\{f(t)\}, \mathcal{L}\{l_n^\alpha(2\lambda t)\} \rangle. \quad (9)$$

The Laplace transform of GLFs can be found in [29]

$$\Lambda_n^\alpha(s) = (2\lambda)^{\frac{1+\alpha}{2}} \left(\frac{1}{s+\lambda}\right)^{1+\frac{\alpha}{2}} \sum_{n=0}^m M_{m,n}^{(\alpha)} \left(\frac{2\lambda}{s+\lambda}\right)^n \quad (10)$$

where $M_{m,n}^{(\alpha)}$ is the matrix given by $M_{m,n}^{(\alpha)} = 0$ for $m < n$, and

$$M_{m,n}^{(\alpha)} = (-1)^n \binom{m}{n} \frac{\Gamma(n+\frac{\alpha}{2}+1)}{\Gamma(n+\alpha+1)} \sqrt{\frac{\Gamma(m+\alpha+1)}{m!}} \quad (11)$$

for $m \geq n$.

According to [14], the scalar product of two functions in the operator domain could be calculated by

$$c_n = \frac{1}{2\pi j} \oint_{\text{RHP}} F(-s) \Lambda_n(s) ds = - \sum_{\text{RHPpoles}} \text{res}\{F(-s) \Lambda_n(s)\}. \quad (12)$$

2.2 Fourier Method to Compute Inverse Laplace Transform

The article [30] described a method of computing the inverse Laplace transform using the Fourier transform. In this paper, s has been substituted by $j\omega$ in the transfer function, and then the transfer function was rewritten into the form

$$F(j\omega) = \frac{M(\omega) + jN(\omega)}{Q(\omega) + jZ(\omega)}. \quad (13)$$

After that, the inverse Laplace transform could be calculated as

$$f(t) = \frac{2}{\pi} \int_0^\infty \frac{M(\omega)Q(\omega) + N(\omega)Z(\omega)}{Q^2(\omega) + Z^2(\omega)} \cos(\omega t) d\omega, \quad (14)$$

or

$$f(t) = -\frac{2}{\pi} \int_0^\infty \frac{N(\omega)Q(\omega) - M(\omega)Z(\omega)}{Q^2(\omega) + Z^2(\omega)} \sin(\omega t) d\omega. \quad (15)$$

2.3 Error Function

The following error function was chosen to compare the solutions:

$$err = \frac{\int_0^T (f_d(t) - f(t))^2 t^2 dt}{\int_0^T f_d^2(t) dt} \quad (16)$$

where $f_d(t)$ is the desired function, and $f(t)$ is the solution.

3. The Design the PID Controllers with the Usage of Generalized Laguerre Functions

In paper [14], the author showed how to employ SLFs to design integer-order PID controllers for integer-order plants. The procedure is based on transforming transfer functions into the SLFs base. In this paper, SLFs will be replaced with GLFs. Furthermore, it will be shown how to use this method for fractional order plants. Unstable systems cannot be directly transformed into GLFs base because an unstable transfer function is not in the L_2 space. Let us assume a system described by the transfer function

$$F_s(s) = \frac{p(s)}{q(s)q_u(s)} \tag{17}$$

where $p(s)$ is the numerator of $F(s)$, $q(s)$ contains only stable poles, and $q_u(s)$ contains unstable poles. This system could be rewritten into

$$F_s(s) = \frac{\frac{p(s)}{q(s)(s+\lambda)^n}}{\frac{q_u(s)}{(s+\lambda)^n}} \tag{18}$$

where n is higher than the order of $q_u(s)$. This description is the fraction of two stable transfer functions, and each could be transformed in the GLFs base. So it could be written into

$$F_s(s) = \frac{\frac{p(s)}{q(s)(s+\lambda)^n}}{\frac{q_u(s)}{(s+\lambda)^n}} = \frac{\sum_{n=0}^{\infty} f_n \Lambda_n^\alpha(s)}{\sum_{n=0}^{\infty} f'_n \Lambda_n^\alpha(s)} \tag{19}$$

If the system $F_s(s)$ is stable, it could be transformed as

$$F_s(s) = \frac{p(s)}{q(s)q_u(s)} = \sum_{n=0}^{\infty} f_n \Lambda_n^\alpha(s) \tag{20}$$

When a controller is designed, many methods seek to match the transfer function of the open loop with the ideal open loop. Open loop $F_0(s)$ is the product of the transfer function of the controller $F_R(s)$ and the transfer function of the plant $F_s(s)$

$$F_0(s) = F_R(s)F_s(s) \tag{21}$$

According to [14], the ideal closed loop is

$$F_c(s) = \frac{\omega_n^2}{s^2 + 2\eta\omega_n + \omega_n^2} \tag{22}$$

where ω_n and η are parameters that have an impact on the final shape of the desired closed loop. The open loop could be derived in the following form:

$$F_0(s) = \frac{\omega_n^2}{s(s + 2\eta\omega_n)} \tag{23}$$

This transfer function is semi-stable, so it should be rewritten into the fraction of two stable transfer functions

$$F_0(s) = \frac{\frac{\omega_n^2}{(s+2\eta\omega_n)(s+\lambda)^2}}{\frac{s}{(s+\lambda)^2}} = \frac{\sum_{n=0}^{\infty} l_n \Lambda_n^\alpha(s)}{\sum_{n=0}^{\infty} l'_n \Lambda_n^\alpha(s)} \tag{24}$$

The transfer function $F_c(s)$ of the PID controller has the following form

$$F_c(s) = k_c \left(1 + \frac{1}{T_i s} + T_d s \right) \tag{25}$$

The transformation of the PID controller transfer function (25) into the GLFs base is

$$F_c(s) = \frac{\frac{k_c(T_i T_d s^2 + T_i s + 1)}{T_i (s+\lambda)^3}}{\frac{s}{(s+\lambda)^3}} = \frac{\sum_{n=0}^{\infty} c_n \Lambda_n^\alpha(s)}{\sum_{n=0}^{\infty} c'_n \Lambda_n^\alpha(s)} \tag{26}$$

The PI controller ($T_d = 0$) could be derived from (25)

$$F_c(s) = k_c \left(1 + \frac{1}{T_i s} \right) \tag{27}$$

The transformation of the PI controller transfer function (27) into the GLFs base is

$$F_c(s) = \frac{\frac{T_i s + 1}{T_i (s+\lambda)^2}}{\frac{s}{k_c (s+\lambda)^2}} = \frac{\sum_{n=0}^{\infty} c_n \Lambda_n^\alpha(s)}{\sum_{n=0}^{\infty} c'_n \Lambda_n^\alpha(s)} \tag{28}$$

Finally, laying ($T_i = \infty$) in (25), the transfer function of the PD controller is

$$F_c(s) = k_c (1 + T_d s) \tag{29}$$

After transforming the transfer function (29) into the GLFs base, it is possible to write

$$F_c(s) = \frac{\frac{T_d s + 1}{(s+\lambda)^2}}{\frac{1}{k_c (s+\lambda)^2}} = \frac{\sum_{n=0}^{\infty} c_n \Lambda_n^\alpha(s)}{\sum_{n=0}^{\infty} c'_n \Lambda_n^\alpha(s)} \tag{30}$$

It is possible to rewrite (21) into the following equation due to the knowledge of approximations of all terms from (21) transformed into the GLFs base

$$\frac{\sum_{n=0}^{\infty} l_n \Lambda_n^\alpha(s)}{\sum_{n=0}^{\infty} l'_n \Lambda_n^\alpha(s)} = \frac{\sum_{n=0}^{\infty} f_n \Lambda_n^\alpha(s)}{\sum_{n=0}^{\infty} f'_n \Lambda_n^\alpha(s)} \frac{\sum_{n=0}^{\infty} c_n \Lambda_n^\alpha(s)}{\sum_{n=0}^{\infty} c'_n \Lambda_n^\alpha(s)} \tag{31}$$

for the unstable system and into

$$\frac{\sum_{n=0}^{\infty} l_n \Lambda_n^\alpha(s)}{\sum_{n=0}^{\infty} l'_n \Lambda_n^\alpha(s)} = \frac{\sum_{n=0}^{\infty} c_n \Lambda_n^\alpha(s)}{\sum_{n=0}^{\infty} c'_n \Lambda_n^\alpha(s)} \sum_{n=0}^{\infty} f_n \Lambda_n^\alpha(s) \tag{32}$$

for the stable system.

From (31) the following expression could be derived for the unstable plant

$$\sum_{n=0}^{\infty} f_n \Lambda_n^\alpha(s) \sum_{n=0}^{\infty} c_n \Lambda_n^\alpha(s) \sum_{n=0}^{\infty} l'_n \Lambda_n^\alpha(s) = \sum_{n=0}^{\infty} f'_n \Lambda_n^\alpha(s) \sum_{n=0}^{\infty} c'_n \Lambda_n^\alpha(s) \sum_{n=0}^{\infty} l_n \Lambda_n^\alpha(s) \tag{33}$$

and from (32) for the stable plant follows

$$\sum_{n=0}^{\infty} f_n \Lambda_n^\alpha(s) \sum_{n=0}^{\infty} c_n \Lambda_n^\alpha(s) \sum_{n=0}^{\infty} l'_n \Lambda_n^\alpha(s) = \sum_{n=0}^{\infty} c'_n \Lambda_n^\alpha(s) \sum_{n=0}^{\infty} l_n \Lambda_n^\alpha(s) \tag{34}$$

The k_c , T_i , and T_d values for the designed PI, PD, or PID controller could be discovered by solving (33) resp. (34). For computations, it is enough to have the first three terms of each series.

3.1 Computation Spectrum Coefficients into GLFs Base

If the plant is described by the integer-order transfer function, spectrum coefficients could be obtained using (12). This is the preferred method because it is possible to get spectrum coefficients analytically. Nevertheless, it is not possible to use residues for fractional-order transfer functions because the term in form

$$\frac{1}{(s + q)^r} \tag{35}$$

where r is not an integer, is not the pole but the essential singularity. On the other hand, it is possible to compute the inverse Laplace transform numerically using (14) and then compute spectrum coefficients in the time domain. This is possible because, according to (9), spectrum coefficients are the same in the time and operator domains. This is not as accurate as the analytical solution using residues because spectrum coefficients are calculated from the approximated impulse response. But as it will be shown in Sec. 4, it is a usable method.

For the term
$$\frac{s^r}{(s + q)^n} \tag{36}$$

where r is not the integer, and n is the integer, it is possible to compute spectrum coefficients using (12) because there is only the pole. That means that for the integer order plant, the integer order open loop, and the integer order controller is beneficial to compute spectrum coefficients in the operator domain using residues according to (12). Table 1 summarizes the domains in which it is beneficial to compute spectrum coefficients.

3.2 Choosing Parameters for GLFs

GLFs have two free parameters, α and λ , which strongly impact the approximation quality. Choosing good values for them is not a trivial problem. In this paper, the MATLAB FMINSEARCH was used. The FMISEARCH minimizes the error function (16). In (16), $f_d(t)$ is the impulse response of the wanted closed loop, and $f(t)$ is the impulse response of the closed loop. This process could be quite time-consuming. Besides, finding optimal values for the free parameters is not trivial. There is no certainty that the values for free parameters that FMISEARCH found are the best.

Coefficients	Integer order	Fractional order
f_n	Operator domain	Time domain
f'_n	Operator domain	Operator domain
l_n	Operator domain	Time domain
l'_n	Operator domain	Operator domain
c_n	Operator domain	Time domain
c'_n	Operator domain	Operator domain

Tab. 1. Domains in which to compute spectrum coefficients.

3.3 Stability of Fractional Order Systems

The method mentioned above does not guarantee the stability of the closed loop. The stability of the closed loop must be analyzed. Stability of the system depends on the roots of the denominator polynomial of the transfer function. For the system with denominator polynomial in form

$$\sum_{n=0}^N a_n s^{nq} \tag{37}$$

we could, according to paper [31], substitute $s^q = F$ so the denominator polynomial will be in form

$$\sum_{n=0}^N a_n F^n. \tag{38}$$

After this transformation all physical roots have angle in $(-q\pi, q\pi)$ and all unstable roots have angle in $(\frac{-q\pi}{2}, \frac{q\pi}{2})$.

3.4 Realization of PID Using Operation Amplifiers

The transfer function of generic inverting amplifier is

$$F_{GA}(s) = -\frac{Z_2}{Z_1} \tag{39}$$

where Z_1 means input impedance and Z_2 means feedback impedance. When Z_1 and Z_2 are both resistors the circuit will be generic inverting amplifier with gain equals to $-\frac{R_2}{R_1}$. When Z_1 is resistor and Z_2 is capacitor the circuit will be integrator with transfer function

$$F_i(s) = -\frac{1}{R_1 C_2 s}. \tag{40}$$

If Z_1 is capacitor and Z_2 is resistor the circuit will be the derivative with transfer function

$$F_d(s) = -C_1 R_2 s. \tag{41}$$

And finally when Z_1 is resistor and Z_2 is parallel connection of resistor and capacitor the final transfer function will be

$$F_a(s) = -\frac{\frac{R_2}{R_1}}{R_2 C_2 s + 1}. \tag{42}$$

From above mentioned circuits it is possible to create integer order PI, PD or PID controllers.

4. Examples

In this section it will be shown that the proposed method works and it will be compared with solutions based on SLFs. In the first example the PI controller for the integer order plant will be tuned. In the second example, the PD controller for the integer order plant will be designed. And finally in the last example it will be shown how to obtain parameters for the PI controller for the fractional order plant.

All Matlab scripts for examples presented in this article are available at [32].

4.1 Example 1

A system in the form

$$F_s(s) = \frac{1}{\frac{1}{3}s + 1} \tag{43}$$

was chosen for the first example. For this system, a PI controller will be designed. For the ideal loop, parameters $\eta = 0.7$ and $\omega_n = 17.14$ rad/s were chosen. The desired open loop is

$$F_0(s) = \frac{293.78}{s(s + 24.00)} \tag{44}$$

and the closed loop is

$$F_c(s) = \frac{293.78}{s^2 + 24.00s + 293.78}. \tag{45}$$

Because $F_s(s)$ is the integer order, all spectrum coefficients could be computed in the operator domain. Spectrum coefficients of the desired open loop and plant transfer function in GLFs and SLFs base are in Tab. 2. The computed parameters are in Tab. 3.

Closed loops were calculated for all designed controllers to analyze the stability according to section 3.3. Systems are of integer order so $q = 1$ and when all poles are in left half of complex plane the system is stable. Transfer functions for each method are shown in Tab. 4. and the stability is discussed.

All designed controllers were simulated in Micro-Cap. Simulation schematic is in Fig. 1. The operational amplifier X_2 realizes the integral part of the PI controller and X_3 realizes the proportional part of the PI controller. From parameters in Tab. 3 and equations (39) to (42) flows that

$$C_1 = \frac{T_i}{R_3 k_c}, \tag{46}$$

$$R_1 = \frac{R_2}{k_c}. \tag{47}$$

Values for resistors R_2 and R_3 were chosen as $R_2 = R_3 = 10$ k Ω . Designed values for all controllers are in Tab. 5.

As you can see from Tab. 3, GLFs offers a slightly smaller approximation error than SLFs. Solutions obtained by SLFs and GLFs both are much better than solution obtained by MATLAB pidtune. Figure 2 shows step responses for comparison. As you can see, the solution with GLFs has smaller overshoot and is slightly faster than the solution with SLFs. This means the quality of the control process is better. Also you can see that simulation in Micro-Cap offers the same results as was calculated in Matlab.

	f_0	f_1	f_2	f'_0	f'_1	f'_2
GLFs	0.4295	0.3994	0.3595	-	-	-
SLFs	1.2161	0.1440	0.0161	-	-	-
	l_0	l_1	l_2	l'_0	l'_1	l'_2
GLFs	0.7343	0.4360	0.2679	-0.0865	-0.0096	0.0239
SLFs	1.0819	-1.2673	-0.0032	0.2299	0.2299	0

Tab. 2. Spectrum coefficients of the open loop and plant.

Method	α	λ	T_i	k_c	err
SLF	0	2.3658	0.3041	3.6697	0.0024
GLF	5.1174	3.4823	0.0901	4.4089	0.0023
MATLAB pidtune	-	-	0.0697	4.450	0.0043

Tab. 3. Parameters for PI controller.

Method	Transfer function	Stability
SLF	$\frac{1.1160s+3.6697}{(s+10.5863)(s+3.4186)}$	Stable
GLF	$\frac{0.3972s+4.4089}{(s+8.1217+9.001j)(s+8.1217-9.001j)}$	Stable
MATLAB pidtune	$\frac{0.3102s+4.450}{(s+6.8362+12.0448j)(s+6.8362-12.0448j)}$	Stable

Tab. 4. Transfer functions of closed loops for PI controllers.

Method	C_1	R_1
SLF	8.2869 μ F	2.725 k Ω
GLF	2.0436 μ F	2.2681 k Ω
MATLAB pidtune	1.5663 μ F	2.2472 k Ω

Tab. 5. Values of components.

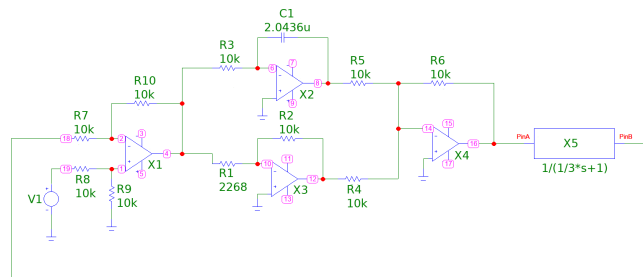


Fig. 1. Simulation schematic for PI controllers.

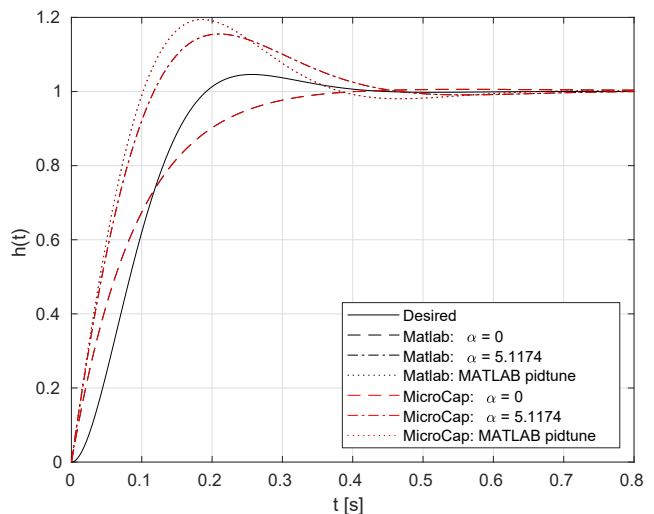


Fig. 2. Step responses of closed loops with PI controller.

4.2 Example 2

A system in the form

$$F_s(s) = \frac{1}{s(\frac{1}{3}s + 1)} \tag{48}$$

was chosen for the second example. For this system, a PD controller will be designed. The realization constant $\epsilon = \frac{T_d}{100}$ for the PD controller was chosen. The parameters $\eta = 0.7$ and $\omega_n = 17.14$ rad/s were selected for the ideal loop. They are the same as in the previous example, so the open loop is described by (44), and the closed loop is described by (45). The plant transfer function is integer-order, thus all computations were made in the operator domain. Spectrum coefficients of the desired open loop and plant transfer function in GLFs and SLFs base are in Tab. 6. Table 7 shows the values of parameters for the desired PD controller.

Closed loops were computed for all designed controllers to analyze stability according to Sec. 3.3. Closed loops in this example are of integer orders so $q = 1$ and when all poles are in left half of the complex plane the system is stable. Transfer functions for each method are shown in Tab. 8 and the stability is discussed.

All designed controllers were simulated in Micro-Cap. Simulation schematic is in Fig. 3. The operational amplifier X_2 realizes the derivative part of the PD controller, X_3 realizes the proportional part of the PD controller and X_6 realizes the realization constant of the PD controller. From parameters in Tab. 7 and equations (39)–(42) flows that

$$C_1 = \frac{T_D}{R_3 k_c}, \tag{49}$$

$$R_1 = \frac{R_2}{k_c}, \tag{50}$$

$$R_{11} = R_{12}, \tag{51}$$

$$C_2 = \frac{T_D}{100R_{12}}. \tag{52}$$

Values for resistors R_2, R_3 and R_{12} were chosen as $R_2 = R_3 = R_{12} = 10$ k Ω . Designed values of the rest components for all controllers are in Tab. 9.

As you can see from Tab. 7, GLFs offer, also in this example, slightly lower approximation error than SLFs, but in Fig. 4 you can see that solutions for GLFs and SLFs are almost the same. Solutions obtained by SLFs and GLFs both are much better than solution obtained by MATLAB pidtune. Also you can see that simulation in Micro-Cap offers the same results as calculated in Matlab.

	f_0	f_1	f_2	f'_0	f'_1	f'_2
GLFs	0.2967	0.1103	-0.0299	0.2463	0.5282	0.2075
SLFs	0.2349	-0.2126	-0.1462	0.3676	0.3676	0
	l_0	l_1	l_2	l'_0	l'_1	l'_2
GLFs	7.0213	2.6762	-0.5650	0.2463	0.5282	0.2075
SLFs	4.1072	-2.7694	-2.2550	0.3676	0.3676	0

Tab. 6. Spectrum coefficients of the open loop and plant.

Method	α	λ	T_d	k_c	err
SLF	0	0.9251	0.2413	15.3404	0.0019
GLF	0.8549	0.5600	0.1668	23.6441	0.0015
MATLAB pidtune	-	-	0.0697	63.80	0.0043

Tab. 7. Parameters for PD controller.

Method	Transfer function	Stability
SLF	$\frac{15.3404+3.7016s}{(s+402.978)(s+9.2976)(s+5.0904)}$	Stable
GLF	$\frac{23.6441+3.9438s}{(s+587.51)(s+7.51+4.01j)(s+7.51-4.01j)}$	Stable
MATLAB pidtune	$\frac{63.80+3.9438s}{(s+1421.3)(s+8.2+11.2j)(s+8.2-11.2j)}$	Stable

Tab. 8. Transfer functions of closed loops for PD controllers.

Method	C_1	R_1	C_2	R_{11}
SLF	370.16 μ F	651.87 Ω	241.3 nF	10.00 k Ω
GLF	394.38 μ F	422.94 Ω	166.8 nF	10.00 k Ω
MATLAB pidtune	444.69 μ F	156.74 Ω	69.70 nF	10.00 k Ω

Tab. 9. Values of components.

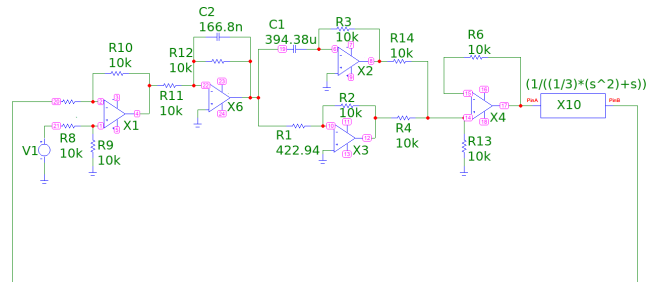


Fig. 3. Simulation schematic for PD controllers.

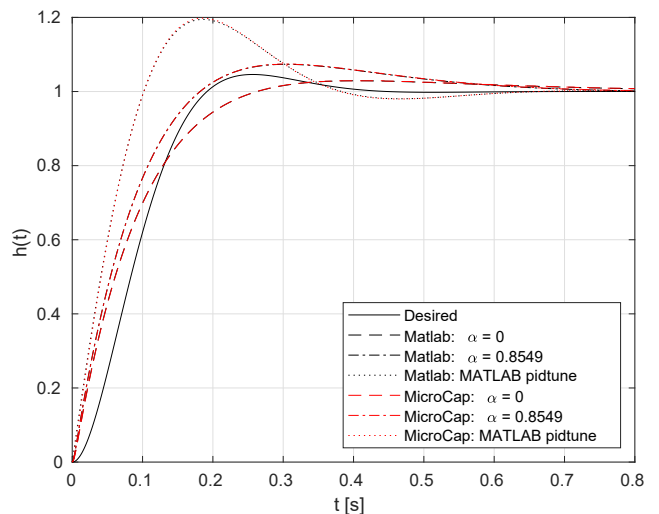


Fig. 4. Step responses of closed loops with PD controller.

4.3 Example 3

Fractional order system with the following transfer function was chosen as the last example

$$F_s(s) = \frac{2}{s^{2.3} + s^{1.4} + 7s^{0.8} + 4}. \tag{53}$$

An integer-order PI controller was designed for this plant. For ideal loop, parameters $\eta = 0.7$ and $\omega_n = 3.2$ rad/s were chosen. The desired open loop is

$$F_0(s) = \frac{10.24}{s(s + 4.48)} \tag{54}$$

and the closed loop is

$$F_0(s) = \frac{10.24}{s^2 + 4.48s + 10.24}. \tag{55}$$

The plant in this example is the fractional-order, thus the spectrum coefficients for the plant were computed in the time domain. The spectrum coefficients of the desired open loop and the plant are in Tab. 10. Values of PI controller parameters are $\alpha = 1.0408 \times 10^{-16}$, $\lambda = 2.9203$, $T_1 = 0.63195$ and $k_c = 4.6079$.

With the designed PI controller the transfer function of closed loop is

$$\frac{5.8239s + 9.2158}{0.63195s^{3.3} + 0.63195s^{2.4} + 4.4237s^{1.8} + 8.3517s + 9.2158}. \tag{56}$$

For the denominator polynomial of the transfer function of the closed loop the largest q is $q = 0.1$. After substitution $s^{0.1} = F$ the denominator polynomial is

$$0.63195F^{33} + 0.63195F^{24} + 4.4237F^{18} + 8.3517F^{10} + 9.2158. \tag{57}$$

This polynomial has 32 roots and only 4 of this roots are physical (according to Sec. 3.3) and have impact on stability. These roots are

$$F_{17,18} = 1.1194 \pm 0.2330j, \\ F_{21,22} = 0.9942 \pm 0.2612j.$$

None of this roots lays in angle region $(-\frac{0.1\pi}{2}, \frac{0.1\pi}{2})$ so the system is stable.

This designed controller was simulated in Micro-Cap. Simulation schematic is in Fig. 1. The transfer function was changed in the block X_5 in conformity with this example. Operational amplifiers X_2 and X_3 have the same meaning as in Example 1. Values for C_1 and R_1 were calculated according to (46) and (47). Values for resistors R_2 and R_3 was chosen $R_2 = R_3 = 10$ k Ω . Calculated values of C_1 and R_1 were $C_1 = 13.715$ μ F and $R_1 = 2.1702$ k Ω .

As you can see in Fig. 5 the results from simulation in Micro-Cap are the same as results computed in Matlab. It is obvious that this method is capable to design PI controllers also for fractional-order plants.

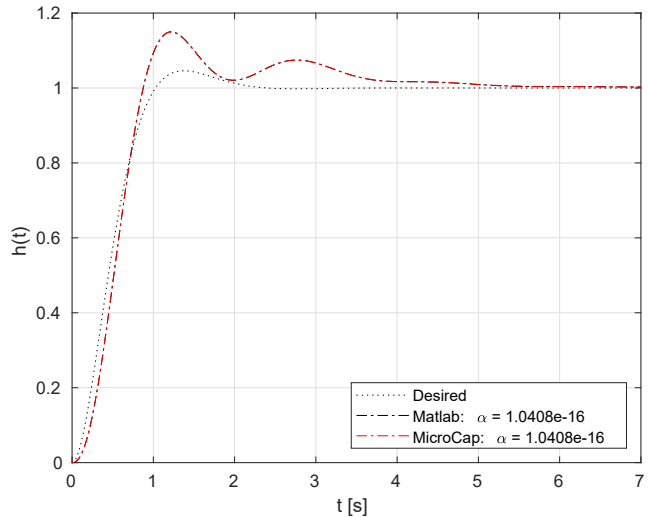


Fig. 5. Step responses of closed loops with PI controller for fractional order plant.

Coefficient	f_0	f_1	f_2	f'_0	f'_1	f'_2
GLFs	0.1315	-0.2016	0.0581	-	-	-
Coefficient	l_0	l_1	l_2	l'_0	l'_1	l'_2
GLFs	0.0980	-0.1754	0.0611	0.2069	0.2069	0

Tab. 10. Spectrum coefficients of the open loop and plant.

5. Conclusion

A method for design of the PID controllers using GLFs was described in this paper. As was shown this method works quite well and is also usable for fractional order systems. This procedure offers better results than the procedure based on SLFs. This method will probably work for design $PI^{\lambda}D^{\eta}$ controllers, but there will be a challenge to choose correct orders for $PI^{\lambda}D^{\eta}$. $PI^{\lambda}D^{\eta}$ controllers could be realized using operational amplifiers when we replace capacitors with constant phase elements designed according to paper [33].

References

- [1] ANNASWAMY, A. M., FRADKOV, A. L. A historical perspective of adaptive control and learning. *Annual Reviews in Control*, 2021, vol. 52, p. 18–41. DOI: 10.1016/j.arcontrol.2021.10.014
- [2] ASTROM, K. J., HAGGLUND T. *PID Controllers: Theory, Design, and Tuning*. Research Triangle Park (North Carolina, USA): ISA - The Instrumentation, Systems and Automation Society, 1995. ISBN: 1556175167
- [3] ZAND, J. P., SABOURI, J., KATEBI J., et al. A new time-domain robust anti-windup PID control scheme for vibration suppression of building structure. *Engineering Structures*, 2021, vol. 244, p. 1–16. DOI: 10.1016/j.engstruct.2021.112819
- [4] GUO, L., ZHANG, J. PID control of nonlinear stochastic systems with structural uncertainties. *IFAC-PapersOnLine*, 2020, vol. 53, no. 2, p. 2189–2194. DOI: 10.1016/j.ifacol.2020.12.002
- [5] MA, D., CHEN, J., LIU, A., et al. Explicit bounds for guaranteed stabilization by PID control of second-order unstable delay systems. *Automatica*, 2019, vol. 100, p. 407–411. DOI: 10.1016/j.automatica.2018.11.053

- [6] YU, H., GUAN, Z., CHEN, T., et al. Design of data-driven PID controllers with adaptive updating rules. *Automatica*, 2020, vol. 121, p. 1–10. DOI: 10.1016/j.automatica.2020.109185
- [7] LEE, Y. W. Synthesis of electric networks by means of the Fourier transforms of Laguerre's functions. *Journal of Mathematics and Physics*, 1932, vol. 11, no. 1–4, p. 83–113. DOI: 10.1002/sapm193211183
- [8] LEE, Y. W. *Statistical Theory of Communication*. John Wiley & Sons Inc., 1960. ISBN: 9780471522065
- [9] AKCAY, H., NINNESS, B. Orthonormal basis functions for modelling continuous-time systems. *Signal Processing*, 1999, vol. 77, no. 3, p. 261–274. DOI: 10.1016/S0165-1684(99)00039-0
- [10] SAMUEL, E. R., FERRANTI, F., KNOCKAERT, L., et al. Reduced order delayed systems by means of Laguerre functions and Krylov subspaces. In *IEEE 18th Workshop on Signal and Power Integrity (SPI)*. Ghent (Belgium), 2014, p. 1–4. DOI: 10.1109/SaPIW.2014.6844545
- [11] HIRAMA, Y., HAMANE, H., HIROKI, F. Closed loop modelling method for non-linear system using Laguerre polynomials. In *International Conference on Control, Automation and Systems (ICCAS)*. Gyeonggi-do (South Korea), 2010, p. 231–236. DOI: 10.1109/ICCAS.2010.5670327
- [12] MALTI, R., EKONGOLO, S. B., RAGOT, J. Dynamic SISO and MISO system approximations based on optimal Laguerre models. *IEEE Transactions on Automatic Control*, 1998, vol. 43, no. 9, p. 1318–1323. DOI: 10.1109/9.718626
- [13] DATTOLI, G., GERMANO, B., RICCI, P. E. Laguerre orthogonal functions from an operational point of view. *Integral Transforms and Special Functions*, 2006, vol. 17, no. 11, p. 779–783. DOI: 10.1080/10652460600856385
- [14] TABATABAEI, M. PID controller design based on Laguerre orthonormal functions. *Journal of Control Engineering and Applied Informatics*, 2016, vol. 18, no. 4, p. 65–76. DOI: 10.1007/s40435-016-0248-8
- [15] OLIVIER, P. D. PID controller design using Laguerre series. In *Proceedings of the 17th Mediterranean Conference on Control and Automation (MED)*. Thessaloniki (Greece), 2009, p. 846–851. DOI: 10.1109/MED.2009.5164650
- [16] WOLFRAM MATH WORLD. *Associated Laguerre Polynomial*. 2017, [Online] Cited 2021-12-19. Available at: <http://mathworld.wolfram.com/AssociatedLaguerrePolynomial.html>
- [17] WOLFRAM RESEARCH. *The Wolfram Functions Site: Polynomials*. 2017, [Online] Cited 2021-12-19. Available at: <http://functions.wolfram.com/Polynomials/>
- [18] NATIONAL INSTITUTE OF STANDARDS AND TECHNOLOGY. *NIST Digital Library of Mathematical Functions: Orthogonal Polynomials*. 2016, [Online] Cited 2021-12-19. Available at: <http://dlmf.nist.gov/18>
- [19] BANERJEE, P. On Galois groups of generalized Laguerre polynomials whose discriminants are squares. *Journal of Number Theory*, 2014, vol. 141, p. 36–58. DOI: 10.1016/j.jnt.2014.01.009
- [20] YADAV M. K. Solutions of a system of forced burgers equation in terms of generalized laguerre polynomials. *Acta Mathematica Scientia*, 2014, vol. 34B, no. 5, p. 1461–1472. DOI: 10.1016/S0252-9602(14)60096-5
- [21] TUMA, M., JURA, P. Dynamical system identification with the generalized Laguerre functions. In *7th International Congress on Ultra Modern Telecommunications and Control Systems and Workshops (ICUMT)*. Brno (Czech Republic), 2015, p. 220–225. DOI: 10.1109/ICUMT.2015.7382431
- [22] TUMA, M., JURA, P. Comparison of different approaches to continuous-time system identification from sampled data. In *European Conference on Electrical Engineering and Computer Science (EECS)*. Bern (Switzerland), 2017, p. 61–65. DOI: 10.1109/EECS.2017.21
- [23] TUMA, M., JURA, P. Dead time estimation in generalized Laguerre functions basis. *AIP Conference Proceedings*, 2020, vol. 2293, no. 1, p. 1–4. DOI: 10.1063/5.0026749
- [24] BJORKLUND S. *Experimental Open-Loop Evaluation of Some Time-Delay Estimation Methods in the Laguerre Domain*. Technical Report, Linköping University, 2003.
- [25] KARSKY, V. An improved method for parameterizing generalized Laguerre functions to compute the inverse Laplace transform of fractional order transfer functions. *AIP Conference Proceedings*, 2020, vol. 2293, no. 1, p. 1–4. DOI: 10.1063/5.0026713
- [26] KARSKY, V., TUMA, M., JURA, P. Approximation of the fractional order transfer functions with integer order transfer functions. *AIP Conference Proceedings*, 2022, vol. 2425, no. 1, p. 1–5. DOI: 10.1063/5.0082206
- [27] KARSKY, V. Parameterizing generalized Laguerre functions to compute the inverse Laplace transform of fractional order transfer functions. *MENDEL - Soft Computing Journal*, 2018, vol. 24, no. 1, p. 79–84. DOI:10.13164/mendel.2018.1.079
- [28] WOLFRAM MATHWORLD. *Gamma Function*. 2022, [Online] Cited 2022-2-17. Available at: <https://mathworld.wolfram.com/GammaFunction.html>
- [29] BELT, H. J. W., BRINKER, A. C. Optimal parametrization of truncated generalized Laguerre series. In *IEEE International Conference on Acoustics, Speech, and Signal Processing (ICASSP)*. Munich (Germany), 1997, p. 3805–3808. DOI: 10.1109/ICASSP.1997.604708
- [30] YUCE, A., DENIZ, F. N., TAN, N., et al. Obtaining the time response of control systems with fractional order PID from frequency responses. In *9th International Conference on Electrical and Electronics Engineering (ELECO)*. Bursa (Turkey), 2015, p. 832–836. DOI: 10.1109/ELECO.2015.7394522
- [31] RADWAN, A. G., SOLIMAN, A. M., ELWAKIL, A. S., et al. On the stability of linear system with fractional-order elements. *Chaos, Solitons & Fractals*, 2009, vol. 40, no. 5, p. 2317–2328. DOI: 10.1016/j.chaos.2007.10.033
- [32] KARSKY, V., TUMA, M. *Design PID Controllers Using Generalized Laguerre Functions - source codes*. 2021, [Online] Cited 2021-12-19. Available at: https://www.vut.cz/www_base/vutdisk.php?i=286301a3f2
- [33] VALSA, J., DVORAK, P., FRIEDL, M. Network model of the CPE. *Radioengineering*, 2011, vol. 20, no. 3, p. 619–626. ISSN: 1805-9600

About the Authors ...

Vilem KARSKY was born in Sumperk, Czech Republic, on July 30, 1992. He received Ing. degree in Electrical Engineering from the Brno University of Technology in Brno, in 2017. Since 2017 he is Ph.D. student at the Dept. of Control and Instrumentation, Brno University of Technology.

Martin TUMA was born in Prague, Czech Republic, on January 20, 1986. He received a Ph.D. degree in Cybernetics, Control and Measurements in 2017. He is a postdoc at the Central European Institute of Technology of Brno University of Technology.